ZnO/FeCo Thin Film Based Tunable Resonator

Jitendra Singh[a)] and Ajay Kumar

Smart Sensors Area, CSIR-Central Electronics Engineering Research Institute Pilani, Rajasthan 333031, India

[a)]Corresponding author: jitendra@ceeri.res.in

Abstract. We have developed a highly Tunable Film Bulk Acoustic Wave Resonator (TFBAR) using magnetostrictive $Fe_{65}Co_{35}$ thin films. The resonator acoustic layer stack consists of ZnO/$Fe_{65}Co_{35}$ layers for tuning of devices. Due to ΔE effect, TFBAR resonance frequency was up-shifted ~106.9MHz (4.91%) in presence of 2kOe magnetic field. From experimental measurement, ΔE enhancement was estimated to be ~35 GPa. Further, it is observed that return loss (S_{11}), phase response and quality factor was improved in presence of magnetic field due to high stiffness of magnetic layer. Equivalent Modified Butterworth-Van Dyke (mBVD) circuit model was developed and fitted with experimental data and circuit parameters are extracted. The proposed resonator is compact, low loss, power efficient and highly tunable. This method also facilitates a new way of tuning FBAR devices using magnetostrictive thin films.

INTRODCTION

Tunable microwave resonator makes microwave transceivers adaptable to multiple bands of operation using a single filter, which is highly desirable in today's communications systems with growing wireless applications. Tunable filters can replace the necessity of switching between several filters to have more than one filter response by inserting tuning elements into a filter topology. Size of RF/Microwave system (cellular radio or mobile phones) is continuously reducing due to a competitive market and therefore the goal is to achieve small size, high performance, and low cost reconfigurable microwave integrated devices. Multiple frequency operations are possible with a single tunable microwave resonator. Currently, acoustic wave resonators are available for single frequency of operation. Recent progress of microwave communication systems indicates that these system has to be more user-friendly i.e. adaptable and reconfigurable. The growing numbers of channels and bandwidth have to be agile (adaptable/reconfigurable). New functionalities are required in devices with superior performance to make them frequency agile and cost-effective.

Film bulk acoustic wave resonator tuning based on magnetostrictive films is rarely investigated. Here, we report new method of tuning FBAR using magnetostrictive $Fe_{65}Co_{35}$ thin films. $Fe_{65}Co_{35}$ thin films show high magnetostrictive coefficient and film Young's modulus can be changed by applied magnetic field.

EXPERIMENTAL PROCEDURE

Magnetic TFBAR was fabricated using a 3-inch diameter double side polished Si(100) wafer using a Silicon bulk micromachining process. Fabrication of TFBAR consists of multiple mask level process. Initially, Si wafers were cleaned using a standard process and loaded in thermal oxidation furnace for growth of silicon dioxide 1.0 μm thickness using a dry-wet-dry process. SiO_2 layer at the back side of wafer was structured using buffered oxide etch BOE process. ZnO layer using a sputter deposition process and patterned by wet chemical etch process. Next, top electrode magnetostrictive $Fe_{65}Co_{35}$ layer was deposited and patterned using a lift-off process to complete the device

Vol. 56(3&4) July & October 2017

circuit. Here, magnetostrictive $Fe_{65}Co_{35}$ layer plays a dual role. This work as top electrode as well as magnetostrictive tuning. Finally, resonator was released using a combination of wet and dry etch processes.

Table I: Material properties of various layers used TFBAR fabrication process.

Material	Young Modulus (GPa)	Density (Kg/m^3)	Poisons ratio (υ)	Acoustic velocity (m/s)	Thickness (μm)
Si	160	2330	0.28	8433	5.0
SiO_2	73.1	2750	0.17	5600	1.0
Pt	168	21450	0.38	3300	0.2
ZnO	211	5680	0.3	6350	1.8
$Fe_{65}Co_{35}$	152	7860	0.27	5900	0.5

RESULTS AND DISCUSSION

Figure 1 shows the scanning electron microscope (SEM) image of a fabricated TFBAR device which was fabricated using a Si bulk micromachining process. Various device layers are clearly noticeable along with electrodes, active area and released cavity area. Active area of resonator comprised of $Pt/ZnO/Fe_{65}Co_{35}$ multilayer stack as emphasized in the Figure 1. The device electrode overlap area was $100\times100\mu m^2$ and designed according to ground-signal-ground (GSG) configuration for on-wafer measurement. The signal line width was 100μm and ground- signal line spacing was 50μm. Magnetic field induced frequency shift was measured using a vector network analyser. The utilized materials properties and thickness parameters are listed in Table I.

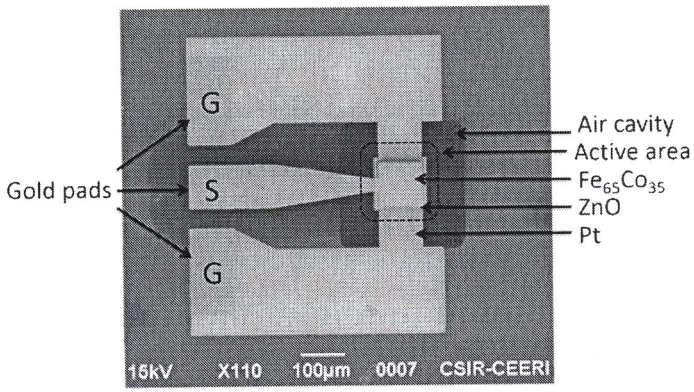

FIGURE 1. Scanning electron microscope (SEM) image of a fabricated TFBAR device and various layer contrast is clearly visible in image.

Figure 2(a) shows the X-day diffraction results of as-deposited $Fe_{65}Co_{35}$ thin films. This indicates that films are polycrystalline in nature and shows only $Fe_{65}Co_{35}$ (200) peak along with Silicon substrate peaks. Magnetic properties of $Fe_{65}Co_{35}$ films were measured using a vibrating sample magnetometer (VSM). Figure 2(b) shows the hysteresis loop of as-deposited $Fe_{65}Co_{35}$ films. Magnetic field was always applied in the plane of film and induced magnetization (emu) was captured by pick-up coils. It is observed that hhysteresis loop was nearly saturated at 2 kOe magnetic field and therefore same field was applied for resonator tuning. Figure 3(a) shows the schematic sketch of resonator measurement set-up. This arrangement consists of magnetic field production source, sample placement stage, gaussmeter and vector network analyzer. Magnetic field was produced using a set of rare earth NeFeB permanent magnets as shown in Fig 3(b). The magnetic field production set-up consists of two rare earth magnets, precision micro-meters, movable trail and sample placement holder. Magnetic field in the range of 100 Oe to 3 kOe can be attained by moving magnet position using precision micro-meters.

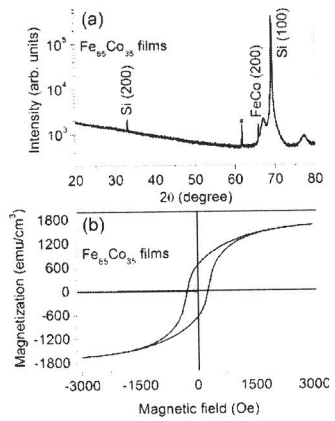

FIGURE 2. (a) X-ray diffraction result of magnetostrictive $Fe_{65}Co_{35}$ films utilized in TFBAR fabrication and (b) In-plane magnetic hysteresis loop of as-deposited $Fe_{65}Co_{35}$ films which was measured by vibrating sample magnetometer (VSM).

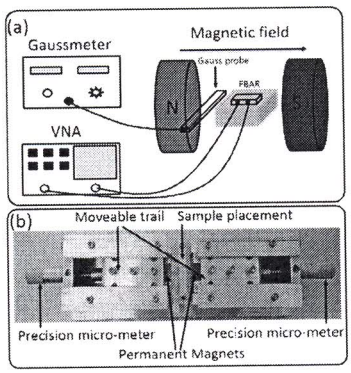

FIGURE 3. (a) Schematics of resonator measurement set-up in presence of dc magnetic field which consists of permanent magnets, Gaussmeter, and vector network analyzer (VNA), (b) In-house developed dc magnetic field source with variable dc magnetic field.

Scattering parameter (S_{11}) of resonator was measured using a vector network analyzer as shown in Figure 4(a). Excitation frequency was sweep in the 1.5 - 3.0 GHz range and resonance peak position was noted. Initially, when there was no magnetic field present, resonance was observed at 2.176 GHz and return loss was -39.5 dB. Correspondingly, phase response was measured and observed that phase change at resonance as shown in Fig.4(b). Now, resonator was placed in dc magnetic field (2kG) as described in Fig. 4(a) and return loss response was measured. It is perceived that resonance frequency was up-shifted to 2.283 GHz and return loss was improved to -45.4 dB. This measured frequency shift was 106.875 MHz and 4.91% of resonance frequency. Here, frequency tuning is very high compared to other reports based on various tuning techniques. As evidence from Fig.4(b) phase response was also improved in presence of magnetic field and sharp at resonance. Resonance frequency (f_a) of tunable resonator is expressed by following eq. (1)

$$f_a = \frac{1}{2d}\sqrt{\frac{E_{eq}}{\rho_{eq}}} \qquad (1)$$

Where d is thickness of piezoelectric ZnO layer, E_{eq} is equivalent Young's modulus of layer stack and ρ_{eq} equivalent layer stack density. When resonator is placed in magnetic field, there is change in resonance frequency and modified frequency (f_p) can be given by following eq. (2)

$$f_p = \frac{1}{2d}\sqrt{\frac{E_{eq} + \Delta E}{\rho_{eq}}} \qquad (2)$$

where ΔE is strain enhanced Young's modulus in presence of magnetic field. Shift in resonance frequency can be given as follows:

$$\Delta f = f_p - f_a = \frac{1}{2d}\left(\sqrt{\frac{E_{eq}+\Delta E}{\rho_{eq}}} - \sqrt{\frac{E_{eq}}{\rho_{eq}}}\right) \qquad (3)$$

where Δf is resonance frequency shift, which was experimentally measured using a vector network analyzer. Equivalent Young's modulus E_{eq} and ρ_{eq} density were estimated by using layer stack physical parameters using a relations $E_{eq} = \sum E_i t_i$ and $\rho_{eq} = \sum \rho_i t_i$, where E_i is Young's modulus and ρ_i is density and t_i is volume fraction of each layer. Piezoelectric layer thickness (d) was measured using experimental procedure during the TFBAR fabrication. Enhanced Young's modulus (ΔE) was estimated from eq. (3), and found to be 35.06 GPa, in presence of 2kG magnetic field. This is considered as a very large change in Young's modulus of $Fe_{65}Co_{35}$ films.

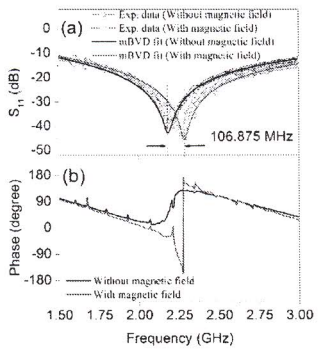

FIGURE 4. (a) Insertion loss curve of TFBAR without magnetic field and in presence of magnetic field and (b) Phase response of resonator without magnetic field and with magnetic field.

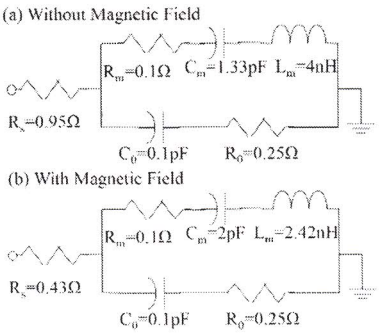

FIGURE 5. Modified Butterworth-Van Dyke (mBVD) model fitting of fabricated TFBAR and mBVD equivalent circuit of the resonator (a) without magnetic field, and (b) in presence of magnetic field.

Table II: Experimental and theoretical parameters of TFBAR.

Parameters	Frequency (GHz)		Return Loss (dB)		Quality factor (Q)	
Magnetic field	Exp.	Theory	Exp.	Theory	Exp.	Theory
No field	2.176	2.182	-39.5	-42.84	64.48	51.95
2000 Oe	2.283	2.285	-45.4	-45.55	81.17	65.28

Due to applied magnetic field, resonance frequency was up-shifted 106.875 MHz (4.91%) and return loss (S_{11}) was improved to -45.4dB. FBAR tuning was achieved 4.91%, which is much higher than other reported values. Without magnetic field quality factor was 64.48 and improved to 81.17 in presence of magnetic field. Series

resistance losses are improved and further quality factor was improved. This improvement in response is attributed to enhancement in stiffness of acoustic layer stack (~35.06 GPa). To understand the basic underlying mechanism, equivalent Modified Butterworth-Van Dyke (mBVD) circuit was developed using Agilent Advanced Design System (ADS) and with fitted model as shown in Figure 5. Result indicates that motional arm capacitance was increased and inductance was decreased in presence of magnetic field due to field induced strain. Moreover, series resistance was decreased (0.95Ω to 0.43Ω) suggests that losses are improved most probably due to high stiffness of $Fe_{65}Co_{35}$ layer in presence of magnetic field. Experimentally measured and theoretically analyzed parameters of TFBAR are compared in Table II. As discussed, tuning behaviors of resonator depends on the magnetostriction coefficient (λ) and is highly tuning devices are possible using high magnetostrictive films. Film bulk acoustic wave resonators are highly sensitive to strains in films. Here, strain induced behavior was used as a basis to tune the resonator. These devices can have various applications in magnetic sensors, actuators and multifunctional reconfigurable microwave devices.

CONLUSIONS

Strain induced TFBAR was realized using magnetostrictive $Fe_{65}Co_{35}$ thin films. When the resonator is subject to magnetic field there is expansion in $Fe_{65}Co_{35}$ layer due to magnetostrictive effect and this expansion leads to a strain in magnetic layer, which alters the magnetic film Young's modulus due to ΔE effect. The proposed resonator is very promising and can be utilized for a variety of reconfigurable microwave resonators, frequencies agile devices and magnetic sensors. This facilitate new method of tuning FBAR devices and new class of reconfigurable devices based on magnetostrictive effect. Variety of tunable devices are possible to realize using magnetostrictive films in MEMS/NEMS technologies.

ACKNOWLEDGMENTS

Authors are thankful to fabrication team at CSIR-CEERI Pilani. This research work was financially supported by the DST - Science and Engineering Research Board, Grant No. EMR/2016/006279.

REFERENCES

1. A. A. Mansour and T.S. Kalkur, IEEE Trans. on Ultrason., Ferroelectr., and Freq. Control **64**, 452 (2017).
2. G. N. Saddik, D. S. Boesch, S. Stemmer, and R. A. York, Appl. Phys. Lett. **91**, 043501 (2007).
3. H. Campanella, J. Esteve, J. Montserrat, A. Uranga, G. Abadal, N. Barniol, and A. Romano-Rodríguez, Appl. Phys. Lett. **89**, 033507 (2006).
4. A. Volatier, E. Defaÿ, M. Aïd, A. N'hari, P. Ancey, and B. Dubus, Appl. Phys. Lett. **92**, 032906 (2008).
5. J. Conde and P. Muralt, IEEE Trans. Ultrason. Ferroelectr. Freq. Control **55,** 1373 (2008).
6. A. Noeth, T. Yamada, P. Muralt, A. K. Tagantsev and N. Setter, IEEE Trans. on Ultrason. Ferroelectr. and Freq. Control **57**, 379 (2010).
7. J. Berge, A. Vorobiev, W. Steichen, and S. Gevorgian IEEE Trans. Microw. Wireless Component Lett. **17**, 655 (2007).
8. J. Kiser, P. Finkel, J. Gao, C. Dolabdjian, J. Li, and D. Viehland, Appl. Phys. Lett. **102**, 042909 (2013).